International Journal of Engineering

Journal Homepage: www.ije.ir

Investigation on Nose and Tail Shape Effects on Hydrodynamic Parameters in Autonomous Underwater Vehicles

S. Abbasi[a], M. Zeinali*[b]

[a] School of Mechanical Engineering, Arak University of Technology, Arak, Iran
[b] School of Mechanical Engineering, Iran University of Science and Technology, Tehran, Iran

PAPER INFO

Paper history:
Received 10 April 2018
Received in revised form 07June 2018
Accepted 22 July 2018

Keywords:
Autonomous Underwater Vehicles
Hull Shape Design
Multi-objective Optimization

ABSTRACT

Development of autonomous underwater vehicles (AUVs) which meets the design constraints and provides the best hydrodynamic performance is really an important challenge in the field of hydrodynamics. In this paper a new profile is used for designing the hull of AUVs. The nose and tail profiles of an AUV using presented profile is designed such that it can properly consider the length constraints due to arrangement of different components in the AUV body. In the current work the flow around an AUV is simulated numerically. Then, the nose and tail profiles are changed in order to investigate the contribution of each of these elements on pressure distribution over the body as well as total drag of the underwater vehicle. The effects of nose and tail profiles on hydrodynamic performance of body were evaluated for this underwater vehicle. Results showed that modified nose and tail shape improved the hydrodynamic behavior of AUVs effectively

***doi**: 10.5829/ije.2018.31.12c.15*

NOMENCLATURE

L	total length of the body (m)	CD_p	pressure drag coefficient
L_n	length of the nose (m)	p	static pressure (Pa)
L_t	length of the tail (m)	U	magnitude of free stream velocity (m/s)
d_n	diameter of nose blunt section (m)	u_i	velocity component in direction i (m/s)
d_t	diameter of tail base section (m)	**Greek Symbols**	
D	body diameter (m)	ρ	Density (kg/m^3)
θ	tail angle	ν	Kinematic viscosity (m^2/s)
CD_f	friction drag coefficient	τ_w	wall shear stress (Pa)

1. INTRODUCTION

About 70% of the earth surface is covered by water, while the need to protect various marine species and utilize energy and mineral resources of seas and oceans have made access to deep seas necessary more than any time before. Autonomous underwater vehicles (AUVs) have shown an undeniable capability to search in the seas, in the past two decades [1]. Therefore, there has been growing researches to design an AUV for performing a desired mission in the deep seas [1]. Reduction of the required energy for movement of the AUV is the most significant objective in hydrodynamic design of the AUV. For this purpose, some methods like optimization of body shape, controlling boundary layer on the body, proper designing of propulsion system and optimal control of movement are used [1]. All the mentioned methods are used in an appropriate design. The body of the AUVs is designed in such a way to provide a better hydrodynamic performance. Therefore, minimum drag force, greater loading capacity, higher speed and larger operation range are the most significant

*Corresponding Author Email: *zeinali@iust.ac.ir* (M. Zeinali)

Please cite this article as: S. Abbasi, M. Zeinali, Investigation on Nose and Tail Shape Effects on Hydrodynamic Parameters in Autonomous Underwater Vehicles, International Journal of Engineering (IJE), IJE TRANSACTIONS C: Aspects Vol. 31, No. 12, (December 2018) 2102-2108

parameters for designing of the AUVs. Meanwhile, cavitation corrosion must be strictly avoided on the body.

Finding the optimal body profile has been always an interesting subject for hydrodynamic experts. Among all activities conducted to propose the body profile for the AUVs, Myring profile is of significant importance [2]. The main reason can be found in successful AUV samples, the body of which are designed and fabricated using the Myring profile. Some of the samples AUVs which have adopted the Myring profile are REMUS underwater vehicle design by Hydroid Institute, ISiMi underwater vehicle manufactured by KORDI Incorporation and MAYA underwater vehicle made by NOI institute [1]. Parsosns et al. [3] suggested a low drag body profile for axisymmetric bodies. They presented the low drag streamlined body profile for incompressible laminar flow. Pinebrook et al. [4] optimized the body profile of an axisymmetric body at zero angle of attack. They used genetic algorithm, for optimization of the body profile with this assumption that there is no separation in the boundary layer. Paster [5] explained how the body design affects reduction of drag, noise, volume and thus fabrication costs. He proposed some methods for estimation of the drag as a function of speed, shape and size. Packwood et al. [6] examined the optimal shape and dimensions of an AUV by applying some initial constraints in accordance with the mission under consideration. Suman et al. [7] assessed hydrodynamic performance of a high speed underwater vehicle with different noses and reported in their results that an elliptical nose provides much better hydrodynamics in comparison with the others. However, when the designers decided to design body of an AUV for practical applications, they have faced some limitations for changing geometrical parameters of the body. The main reason was the constraints the designers experience due to arrangement of different components in the AUV body. Thus, new algorithms are being developed in every day which take into account these constraints for designing the body [7].

This paper has provided a general profile to design the body shape of AUVs by considering the body geometrical constraints. Generally, one may simply take into consideration the length limitations arisen due to structural design of the body. In the following, this paper will investigate the effects of changing the nose and tail profile on the hydrodynamic behavior of the AUV and evaluate the contribution of the nose and tail profiles in the total drag of the body using numerical simulation

2. AUV GEOMETRICAL SPECIFICATIONS

Figure 1 depicts a schematic view of an AUV with its general specifications. As can be seen from the general specifications of this AUV, some characteristic lengths have been defined for the general shape of the body so as to arrange the different components inside the AUV body. Table 1 represents these specified lengths include the total length of the body (L) in 500 mm diameter (D), length of the nose (L_n), length of the tail (L_t), diameter of nose blunt section (d_n) and diameter of tail base section (d_t).

In the current work a general equation compatible with the geometric constraints of the body structural design has been proposed to study the effect of nose and tail profiles on total drag of the AUV body. Equation (1) was used to determine the nose profile. It would be possible to generate different profiles based on the suggested equation.

$$Y(X_n)=(D-d_n)\left(\begin{array}{l}A_n\left[\frac{X_n}{L_n}\right]^{\alpha_n}\\ +B_n\left[\frac{X_n}{L_n}\right]^{\beta_n}\\ +C_n\left[\frac{X_n}{L_n}\right]^{\gamma_n}\end{array}\right)+\frac{dn}{2} \quad (1)$$

Equation (2) has been used to determine the tail profiles:

$$Y(X_t)=(D-d_t)\left(\begin{array}{l}A_t\left[\frac{X_t}{L_t}\right]^{\alpha_t}\\ +B_t\left[\frac{X_t}{L_t}\right]^{\beta_t}\\ +C_t\left[\frac{X_t}{L_t}\right]^{\gamma_t}\end{array}\right)+\frac{D}{2} \quad (2)$$

The algorithm to determine the unknown coefficients to develop the desirable profile for nose or tail can be summarized in Figure 2. By using presented algorithm for producing profiles for nose or tail, various profiles are generated using the selected coefficients. Since designers can consider a profile based on the structural design constraints.

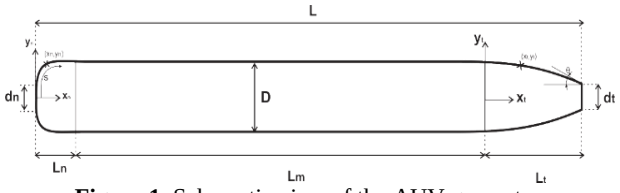

Figure 1. Schematic view of the AUV geometry

TABLE 1. Dimensions and geometries of the AUV

Parameter	D	L	L_n	L_m	L_t	d_n	d_t
Value	500	6070	380	4360	1330	265	160

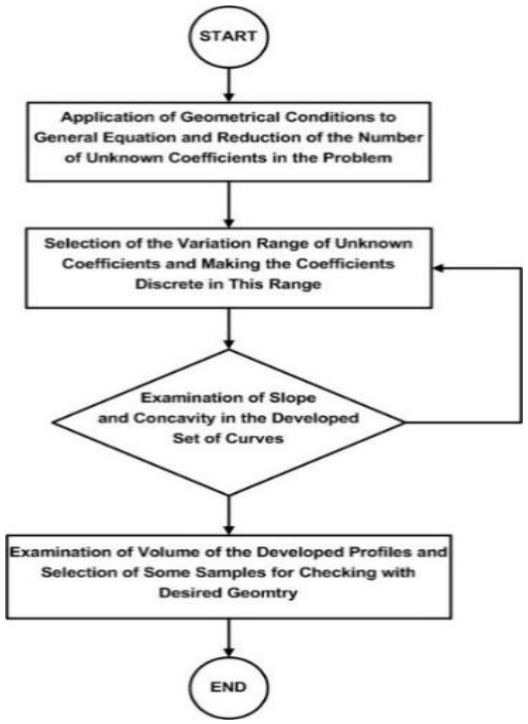

Figure 2. A flowchart for generating desired profile for nose or tail

The nose and tail profile of the AUV was generated using the presented profile. The profile coefficients considered for the nose and tail profiles of the AUVare summarized in Table 2.

Considering a certain profile for nose and tail of the AUV numerical simulation is done at Reynolds number of 3.0×10^7. The nose and tail profiles are changed and then simulations are done to evaluate the effects of changing the nose and tail profiles on pressure distribution around the AUVand also on drag force of the body under study.

TABLE 2. Profile coefficients considered for nose and tail of the AUV

Nose Profile coefficients		Tail Profile coefficients	
A_n	**1.3**	A_t	**-0.125**
B_n	**4.2**	B_t	**0.375**
C_n	**-5**	C_t	**-0.75**
α_n	**0.6**	α_t	**4.8**
β_n	**1.5**	β_t	**4.2**
γ_n	**1.6**	γ_t	**2.6**

3. FLOW SIMULATION

In the present investigation finite volume scheme was used for solution of governing equations of continuity and momentum for an incompressible flow [8].

To evaluate numerical schemes the existing experimental results for the body of DARPASuboff submarine have been taken as a benchmark [9]. Fluent software was used for the numerical simulation of DARPASuboff submarine at Reynolds number of 1.2×10^7. Distribution of pressure coefficient (Cp) around the body of DARPASuboff has shown in the following figure and the results obtained from the simulations have been compared with the experimental results.

The results obtained from the simulations and their comparison with the experimental results indicates that using an average mesh of 40,000 number and y+ of the first mesh being 30, one can attain accurate results.

In the current work, an axisymmetric problem with appropriate boundary conditions is solved over a finite computational domain. The computational domain extended 1L upstream of the leading edge of the axisymmetric body, 1L above the body surface and 5L downstream from the trailing edge. Here L is thelength of the body shown in Figure 4.

The solution was evaluated on a structured mesh. For the current work, it was found that a grid size of 60,000 cells was sufficient for the simulations, with the first grid point being located at $y^+ \approx 30$.

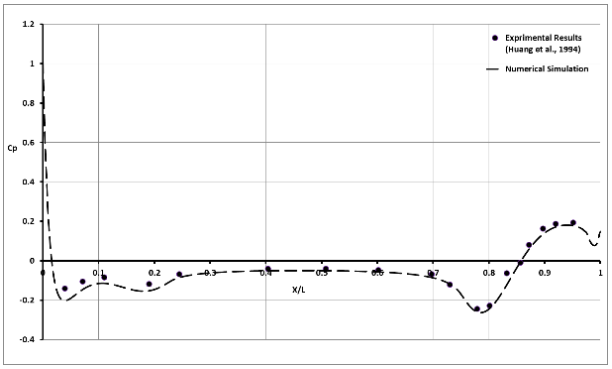

Figure 3. Effect of number of mesh on distribution of Cp and Cf around DARPASuboff body

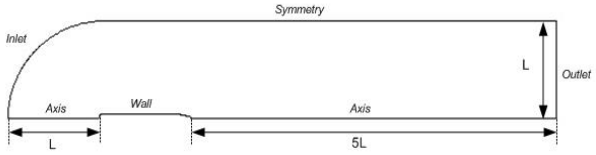

Figure 4. Computational domain and boundary conditions

So in combination with the turbulence model, a wall function based on the law of the wall is used [10]. A typical grid layout near the body is shown Figure 5.

For numerical simulation, the SIMPLE algorithm was used to compute the pressure field. Numerical schemes for the transported turbulent quantities were set to first-order upwind, and they are set to second-order central schemes for the pressure and velocity. The simulation is conducted at Reynolds number of 3.0×10^7. Where Reynolds number is given by:

$$\mathrm{Re}=\frac{U\,L}{\nu} \tag{1}$$

where, U is magnitude of free stream velocity, L is the AUV length, and ν is the fluid kinematic viscosity. Figure 6 shows contours of pressure field and the pressure distribution around the body obtained from numerical simulation.

4. RESULTS AND DISCUSSION

Some sample profiles were considered for nose and tail of the AUV in order to examine the role of nose and tail profiles in total drag of the body, and then the effect of each profile on hydrodynamic behavior of the body was evaluated.

To perform the numerical simulation, meshing and numerical settings similar to simulation of initial body of the AUV were used for all the samples. In all of these simulations, the same type of profile was used for the tail of the AUV.

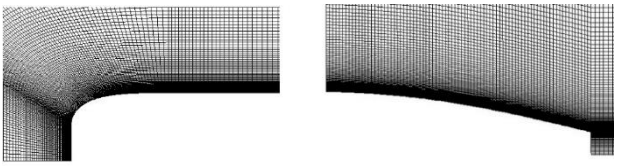

Figure 5. Schematic view of the grid around body

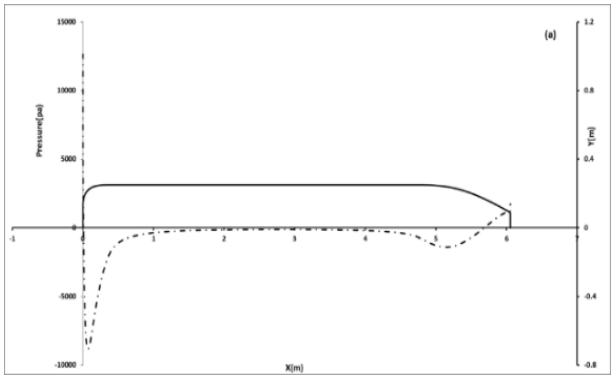

Figure 6. Contours of pressure field and Distribution of pressure around body

The results obtained from these simulations are given in the Table 3. Some results like contribution of pressure drag and friction drag in total drag of the body as well as the contribution of the pressure and friction drag of the nose in the nose drag were provided.

The total drag coefficient on a body is usually considered consist of friction drag coefficient and pressure drag coefficient calculated as follows:

$$CD=CD_f+CD_p \tag{2}$$

Where CD_f is friction drag coefficient and CD_p is pressure drag coefficient and are given below:

$$CD_f=\frac{\left(\int_A \tau_w dA\right)\hat{i}}{0.5\rho U^2 A_f},\quad CD_p=\frac{\left(\int_A pdA\right)\hat{i}}{0.5\rho U^2 A_f} \tag{5}$$

where, τ_w Is wall shear stress, A is body wetted area, A_f is AUV frontal area, p is static pressure, U is flow free stream velocity, ρ is fluid density and $\hat{i}$ is unity vector parallel to flow direction.

It can be seen from the Table 4 that the pressure drag is approximately made up 15-20% of the total drag associated with the AUV body. On the other hand, the friction drag comprises up to 80% of the total drag of the body. This finding makes clear the significant importance of using different methods for reduction the friction drag of AUVs. The ratio of nose pressure drag to body pressure drag is indicative of this fact that the nose has a greater share of the pressure drag (i.e. 60-70%). Therefore, in AUVs like that of current case, a greater care must be taken on nose profile for minimization of the pressure drag on the body. Moreover, it can be inferred from the obtained results that by reducing the volume related to the nose, contribution of the nose pressure drag has decreased as compared to that of the nose friction drag.

It can be seen from the Table 4 that the pressure drag is approximately made up 15-20% of the total drag associated with the AUV body. On the other hand, the friction drag comprises up to 80% of the total drag of the body. This finding makes clear the significant importance of using different methods for reduction the friction drag of AUVs. The ratio of nose pressure drag to body pressure drag is indicative of this fact that the nose has a greater share of the pressure drag (i.e. 60-70%). Therefore, in AUVs like that of current case, a greater care must be taken on nose profile for minimization of the pressure drag on the body. Moreover, it can be inferred from the obtained results that by reducing the volume related to the nose, contribution of the nose pressure drag has decreased as compared to that of the nose friction drag.

Distributions of the pressure around bodies of some samples are shown in Figure 7. As can be observed from this figure, changing of the noses has no effect on the pressure distribution on tail of the AUV. As evident in this figure, the nose profile of the sample which has the smallest volume among the samples under study represents the minimum pressure drop and this reduces the probability of cavitation occurrence on the nose of AUV.

Moreover, based on this figure and the results from Table 3 it can be found out that by increasing the pressure drag of the nose the minimum pressure on the nose has reduced which can increase the possibility of cavitation occurrence on front of the nose. In other words, for the samples which have the minimum pressure drag, the cavitation is less likely to occur.

According to this figure in the samples under study amount of pressure drop has increased by increasing of the volume or better to say increasing of the curvature of the nose profile can finally shift location of the minimum pressure ahead the nose. The values of friction, pressure, and total drag coefficients for different noses are illustrated in Figure 8 versus the volume change caused by them.

One can see that increasing the nose volume does not change the friction drag coefficient significantly, but the pressure drag coefficient is increased, which leads to a greater total drag coefficient for the nose when the nose volume is increased.

Some sample profiles were selected in this section for evaluation of the effects of changing the tail on hydrodynamic behavior of the AUV. As can be observed in Table 4, changing of the tail profile in the AUV puts a small effect on the amount of total drag coefficient. Based on these results, increasing of the tail volume adds to the contribution of the tail friction drag coefficient, while the contribution of the tail pressure drag coefficient decreases slightly. Distributions of the pressure around body of the some simulated samples are shown in Figure 9.

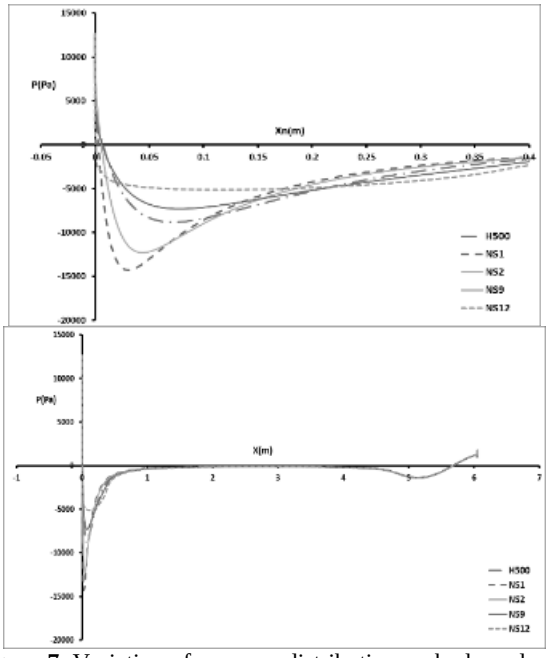

Figure 7. Variation of pressure distribution on body and nose of the AUV by changing of tail profile

TABLE 3. Effect of changing nose profile in coefficient of total drag of the AUV body

Case	CD_{Body}	$\frac{CD_{pBody}}{CD_{Body}}(\%)$	$\frac{CD_{pNose}}{CD_{pBody}}(\%)$	$\frac{CD_{fBody}}{CD_{Body}}(\%)$	$\frac{CD_{fNose}}{CD_{fBody}}(\%)$	CD_{Nose}	$\frac{CD_{pNose}}{CD_{Nose}}(\%)$	$\frac{CD_{pNose}}{CD_{Nose}}(\%)$
H500	0.1260	16.42	66.88	83.58	12.75	0.0273	50.74	49.26
NS1	0.1311	19.92	73.93	80.08	13.19	0.0331	58.22	41.78
NS2	0.1291	18.53	71.49	81.47	13.05	0.0308	55.47	44.53
NS3	0.1288	18.39	71.69	81.61	13.02	0.0307	55.38	44.62
NS4	0.1267	16.88	68.55	83.12	12.84	0.0282	52.02	47.98
NS5	0.1281	17.91	70.26	82.09	12.96	0.0298	54.19	45.81
NS6	0.1278	17.77	70.47	82.23	12.93	0.0296	54.09	45.91
NS7	0.1261	16.64	67.96	83.36	12.72	0.0276	51.62	48.38
NS8	0.1254	16.13	66.74	83.87	12.65	0.0268	50.36	49.64
NS9	0.1244	15.37	64.77	84.63	12.5	0.0255	48.49	51.51
NS10	0.1236	14.96	62.97	85.04	12.3	0.0246	47.4	52.60
NS11	0.123	14.73	62.84	85.27	12.23	0.0243	47.04	52.96
NS12	0.1230	14.61	62.45	85.36	12.18	0.0240	46.73	53.27

As can be observed in Table 4, changing of the tail profile in the AUV puts a small effect on the amount of total drag coefficient. Based on these results, increasing of the tail volume adds to the contribution of the tail friction drag coefficient, while the contribution of the tail pressure drag coefficient decreases slightly.

Figure 9 illustrates that changing of the tail profile has no effect on the pressure distribution on the AUV nose. In the Figure 10, the total, pressure and friction drag of the tail have been shown for different samples. As can be observed from Figures 9, 10 and Table 4, increasing the tail volume leads to greater slopes of tail profile. This can increase the positive pressure gradient on the tail and this increases the pressure behind the body which will reduce the pressure drag coefficient related to the tail. However, by increasing the tail wetted area, the friction drag associated with the tail has increased. Meanwhile, it can be understood from these diagrams that increasing the tail volume causes the growth in the tail friction drag to become greater than the reduction in its pressure drag. Therefore, increasing the tail volume will add to the magnitude of tail drag.

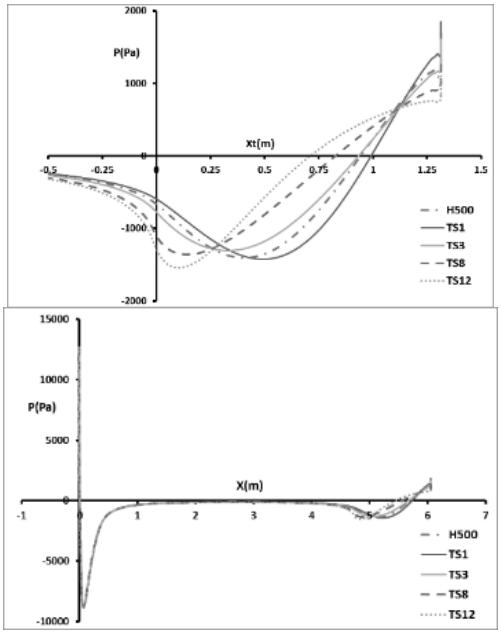

Figure 9. Variation of pressure distribution on body and tail of the AUV by changing of tail profile

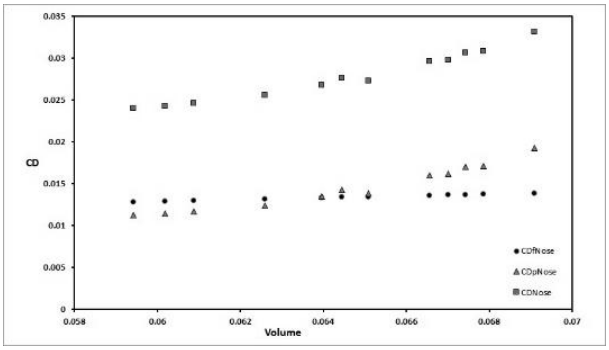

Figure 8. Variation of pressure, friction and total no drag coefficients in different examined samples

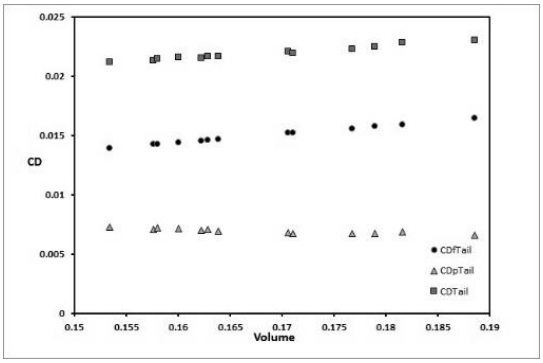

Figure 10. Variation of pressure, friction and total tail drag coefficients in different examined samples

TABLE 4. Effect of changing tail profile on total drag coefficient of the AUV

Case	CD_{Body}	$\frac{CD_{pBody}}{CD_{Body}}(\%)$	$\frac{CD_{pTail}}{CD_{pBody}}(\%)$	$\frac{CD_{fBody}}{CD_{Body}}(\%)$	$\frac{CD_{fTail}}{CD_{fBody}}(\%)$	CD_{Tail}	$\frac{CD_{pTail}}{CD_{Tail}}(\%)$	$\frac{CD_{fTail}}{CD_{Tail}}(\%)$
H500	0.1260	16.42	33.12	83.58	15.12	0.0228	30.07	69.93
TS1	0.1262	16.19	32.27	83.81	15.52	0.0230	28.66	71.34
TS2	0.1257	16.34	32.62	83.66	14.97	0.0225	29.85	70.15
TS3	0.1256	16.35	32.65	83.65	14.84	0.0223	30.07	69.93
TS4	0.1253	16.42	32.86	83.58	14.51	0.0220	30.80	69.20
TS5	0.1261	16.36	33.02	83.64	14.45	0.0221	30.88	69.12
TS6	0.1250	16.61	33.50	83.39	14.07	0.0216	32.17	67.83
TS7	0.1247	16.42	34.52	83.58	14.02	0.0217	32.61	67.39
TS8	0.1250	16.64	33.60	83.36	13.98	0.0215	32.42	67.58
TS9	0.1250	16.77	34.10	83.23	13.85	0.0216	33.15	66.85
TS10	0.1249	16.82	34.31	83.18	13.73	0.0215	33.57	66.43
TS11	0.1248	16.73	33.91	83.27	13.72	0.0213	33.19	66.81
TS12	0.1247	16.90	34.52	83.10	13.44	0.0212	34.31	65.70

5. CONCLUSION

In this work using numerical method, role of the nose and tail profiles in total body drag of an AUV was evaluated. Considering the initial body design of the AUV, a special profile was needed to be able to take into account length constraints due to the body structural design properly.

Thus, a general equation capable of considering the design constraints was proposed. Having applied the suggested algorithm to generate desired profile for nose or tail of the AUV, number of the unknown coefficients of this general equation decreases. Then, the presented equation was used to generate various profiles in a certain length. Studying the hydrodynamic performance of the body of the AUV by numerical simulation reveals that the friction drag has much greater share of the total body drag in comparison with the pressure drag. Moreover, presented results showed the drag of nose as well as the pressure drop of nose head can be reduced by modifying the nose profile, so the probability of cavitation occurrence can be decreased. This will require using a nose with smaller volume. Investigation of the changes in the tail profile indicates that increasing of the tail volume will increase total drag of the tail in spite of tail pressure drag reduction. Accordingly, by decreasing tail wetted area tail contributing in body total drag is reduced.

6. REFERENCES

1. Nouri, N., Zeinali, M. and Jahangardy, Y., "Auv hull shape design based on desired pressure distribution", ***Journal of Marine Science and Technology***, Vol. 21, No. 2, (2016), 203-215.
2. Myring, D., "A theoretical study of body drag in subcritical axisymmetric flow", ***The Aeronautical Quarterly***, Vol. 27, No. 3, (1976), 186-194.
3. Parsons, J.S., Goodson, R.E. and Goldschmied, F.R., "Shaping of axisymmetric bodies for minimum drag in incompressible flow", ***Journal of Hydronautics***, Vol. 8, No. 3, (1974), 100-107.
4. Pinebrook, W.E. and Dalton, C., "Drag minimization on a body of revolution through evolution", ***Computer Methods in Applied Mechanics and Engineering***, Vol. 39, No. 2, (1983), 179-197.
5. Paster, D., "Importance of hydrodynamic considerations for underwater vehicle design", in OCEANS'86, IEEE. Vol., No. Issue, (1986), 1413-1422.
6. Packwood, A. and Huggins, A., "Afterbody shaping and transition prediction for a laminar flow underwater vehicle", ***Ocean engineering***, Vol. 21, No. 5, (1994), 445-459.
7. Suman, K., Rao, D.N., Das, H. and Kiran, G.B., "Hydrodynamic performance evaluation of an ellipsoidal nose for a high speed under water vehicle", ***Jordan Journal of Mechanical & Industrial Engineering***, Vol. 4, No. 5, (2010).
8. Launder, B.E. and Spalding, D.B., The numerical computation of turbulent flows, in Numerical prediction of flow, heat transfer, turbulence and combustion. 1983, Elsevier.96-116.
9. Huang, T. and Liu, H., "Measurements of flows over an axisymmetric body with various appendages in a wind tunnel: The darpa suboff experimental program", Vol., No., (1994).
10. Shih, T.-H., Liou, W.W., Shabbir, A., Yang, Z. and Zhu, J., "A new k-ϵ eddy viscosity model for high reynolds number turbulent flows", ***Computers & Fluids***, Vol. 24, No. 3, (1995), 227-238.

Investigation on Nose and Tail Shape Effects on Hydrodynamic Parameters in Autonomous Underwater Vehicles

S. Abbasi[a], M. Zeinali[b]

[a] School of Mechanical Engineering, Arak University of Technology, Arak, Iran
[b] School of Mechanical Engineering, Iran University of Science and Technology, Tehran, Iran

P A P E R I N F O

Paper history:
Received 10 April 2018
Received in revised form 07June 2018
Accepted 22 July 2018

Keywords:
Autonomous Underwater Vehicles
Hull Shape Design
Multi-objective Optimization

چکیده

توسعه وسایل زیرسطحی خودکنترل که بهترین عملکرد هیدرودینامیکی را داشته باشد یک چالش مهم در حوزه هیدرودینامیک است. در مقاله حاضر یک پروفیل جدید جهت طراحی بدنه وسایل زیرسطحی خودکنترل به کار گرفته شده است. با استفاده از پروفیل حاضر، دماغه و دم یک وسیله زیرسطحی خودکنترل به گونه ای طراحی شده است که به خوبی می تواند قیود طولی ناشی از جانمایی قطعات مختلف در داخل بدنه وسیله زیرسطحی خودکنترل را لحاظ می کند. در کار حاضر جریان حول بدنه وسیله زیرسطحی خودکنترل به روش عددی مورد بررسی قرار گرفته است. در ادامه پروفیل های دماغه و دم به منظور ارزیابی سهم هریک از قسمت ها در توزیع فشار حول بدنه و همچنین درگ کلی وسیله زیرسطحی تغییر داده شده‌اند. و تاثیرات پروفیل دماغه و دم روی عملکرد هیدرودینامیکی بدنه وسیله زیرسطحی خودکنترل ارزیابی شده است. نتایج نشان می دهند که تغییر شکل دماغه و دم به طور موثری رفتار هیدرودینامیکی وسیله زیرسطحی خودکنترل را بهبود می بخشد.

***doi**: 10.5829/ije.2018.31.12c.15*